16 Rainfall on a Slope

16.1 Problem Statement

In this example, the stability of a generic slope is analyzed for two successive rainfall events of increasing intensity and decreasing duration. The slope geometry and location of the initial water table are shown in Figure 16.1. In the first rainfall event, 23 inches (584 mm) of rain accumulate over a period of seven months. In the second event, nine inches (228 mm) of rain fall within four days. The purpose of this analysis is to determine the effect of each event on the stability of the slope.

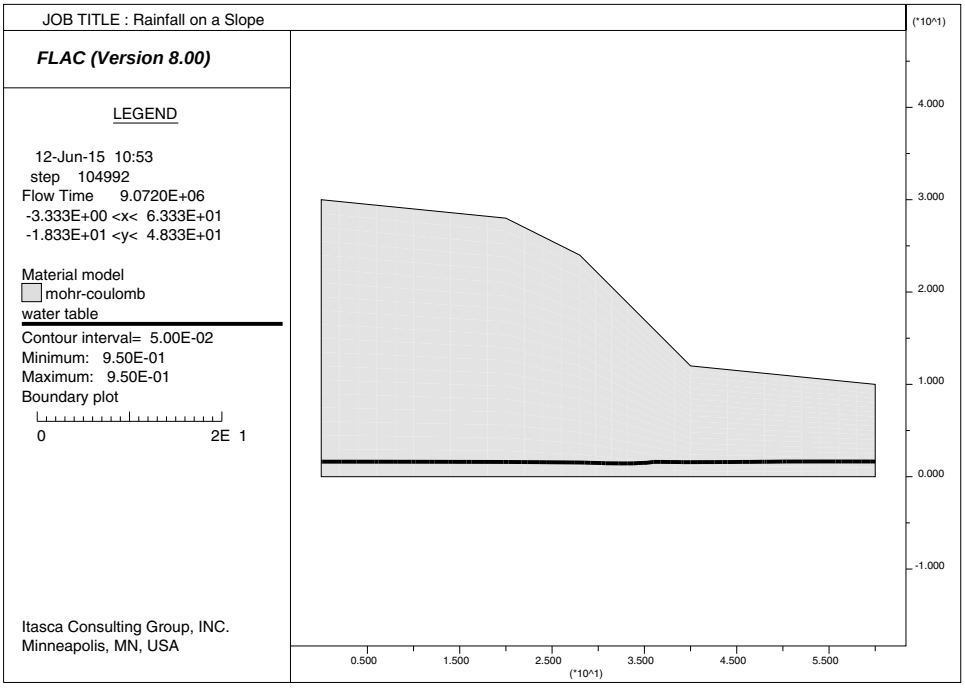

Figure 16.1 Slope with initial water table

16.2 Theoretical Framework

The presence of capillary pressure in unsaturated soils can have a big impact on the stability of a slope. Capillary forces hold fine particles together, and can provide additional cohesion to the soil. The apparent cohesion provided by the capillary forces usually decreases as the soil saturation increases. While a rainfall event of low intensity and long duration may, under certain conditions, be beneficial to the stability of the slope, a high-intensity, short-duration event may promote a buildup of saturation and induce slope failure. This example illustrates the dependency of the rate of infiltration from precipitation on the stability in a generic silty slope.

Unconfined groundwater in soil is usually characterized by the occurrence of a capillary zone in which the soil is not fully saturated. A common assumption in the study of fluid flow in unconfined aquifers is that air is at constant atmospheric pressure in the void space; water is then the only fluid of concern in the formulation. Capillary effects are not considered in the *FLAC* standard fluid-flow logic. To account for capillarity, we use the capabilities of the two-phase flow logic described in Section 2 in **Fluid-Mechanical Interaction**. We model unsaturated groundwater flow by considering a bulk modulus value for the non-wetting air phase several orders of magnitude smaller than the water bulk modulus, thereby preventing any significant generation of air pressure.

The two-phase flow logic uses an extended form of Darcy law for fluid transport, with permeability as an empirical function of saturation. Also, pore pressure in the unsaturated zone is negative, and related to saturation by an empirical law. Both permeability and capillary pressure laws are of the van Genuchten form, commonly assumed for soils. In addition, fluid mechanical coupling is performed based on Bishop effective stress. See Section 2.2 in **Fluid-Mechanical Interaction** for a detailed description of the fluid-mechanical coupling.

16.2.1 Apparent Cohesion

Consider the case of a Mohr-Coulomb material, partially saturated with water. When two-phase flow logic is active, the yield criterion in *FLAC* is

$$\tau^{max} = \sigma^b \tan\phi + C \tag{16.1}$$

where τ^{max} is the material shear strength, σ^b is the Bishop effective stress (compression positive), C is cohesion, and ϕ is friction angle. The Bishop effective stress is defined as

$$\sigma^b = \sigma - (S_w P_w + S_a P_a) \tag{16.2}$$

where σ is the total stress, S_w is water saturation, $S_a = 1 - S_w$ is air saturation, and P_w and P_a are water and air pressure, respectively. After substitution of Eq. (16.2) into Eq. (16.1), and some manipulation, the yield criterion may be expressed as

$$\tau^{max} = (\sigma - P_a)\tan\phi + S_w(P_a - P_w)\tan\phi + C \tag{16.3}$$

As may be seen from this formula, the classical Mohr-Coulomb criterion is recovered when the soil is completely dry initially, or when water saturation, S_w, reaches 1. In unsaturated conditions, the term $S_w(P_a - P_w)\tan\phi$ plays the role of an additional cohesion C_c provided to the soil by the capillary forces. Capillary pressure is defined as $P_c = P_a - P_w$, and the cohesion, C_c, may be expressed as

$$C_c = S_w P_c \tan\phi \tag{16.4}$$

Capillary pressure is a decreasing function of saturation; it is represented in *FLAC* by an empirical law of the van Genuchten form (see Section 2.2.1 in **Fluid-Mechanical Interaction**):

$$P_c = P_0\left[S_e^{-1/a} - 1\right]^{1-a} \tag{16.5}$$

where S_e is the effective saturation, and P_0 and a are parameters to be determined experimentally. The parameter P_0 gives a measure of the soil capillary strength, and is higher for fine-grained material. The parameter a characterizes the slope of the capillary curve; it is close to 1 for poorly graded soils, and close to zero for well-graded soils. The function P_c/P_0 is plotted versus effective saturation, S_e, for different values of a (0.336 and 0.6) in Figure 16.2. The function $C_c/(P_0 \tan\phi)$ is plotted versus effective saturation for the same values of a in Figure 16.3.

Typical capillary curves for soils can be found in Bear (1979) – e.g., see Figure 6-9, p. 199. The solid curve in Figure 16.2 (a = 0.336) is representative of a silty material, and the dashed curve (a = 0.6) is representative of sand. The capillary curve for silty material indicates that, once the soil has been wetted, it is very difficult to extract back the last drop of water. This is the type of soil we are considering in this simulation example. In Figure 16.3, the scaled cohesion $C_c/(P_0 \tan\phi)$ is plotted versus saturation for the same values of a.

For soils characterized by a coefficient, $a > 0.5$, there is, according to the equations considered above, an optimal saturation that offers the most cohesive strength to the material (see the dashed curve in Figure 16.3). This would be the case for a damp sand castle on the beach (C = 0). If the sand is too damp or too dry, the castle will not be able to keep its shape, and will collapse. For types of soil with $a \leq 0.5$ (e.g., the solid curve in Figure 16.3), a small amount of humidity is enough to provide substantial additional cohesive strength to the soil. This could be the case for silt, for example.

In both cases, if soil saturation becomes sufficiently high, the soil cohesion, C_c, is predicted to decrease. In the case of a slope, the increase in saturation may occur, for example, after a heavy rain, and this may lead to slope collapse under certain conditions.

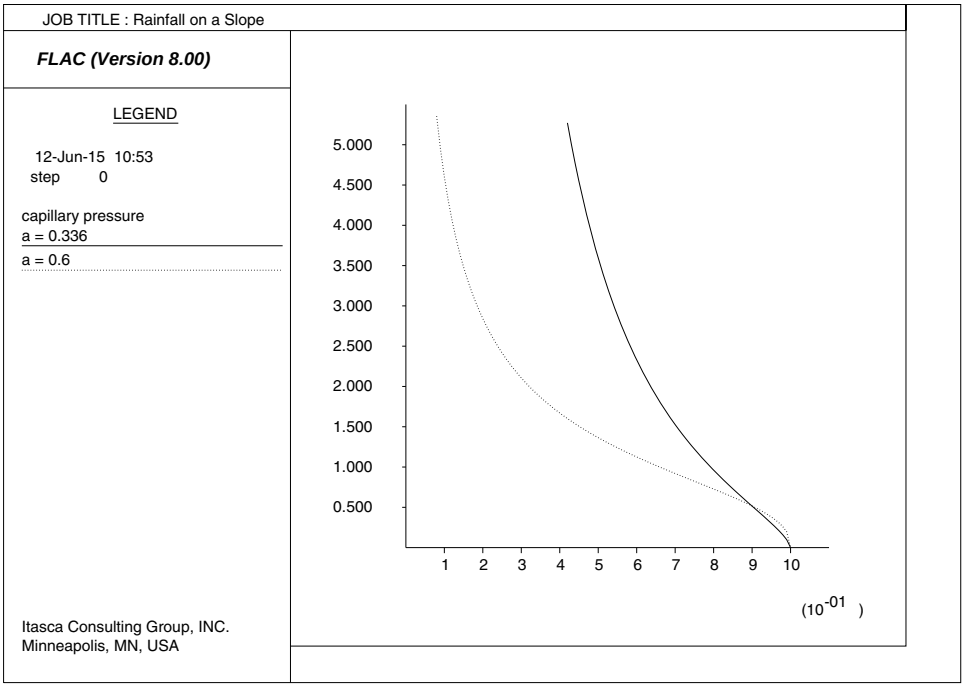

Figure 16.2 Capillary curves, P_c/P_0 versus effective saturation, S_e, for a = 0.336 and a = 0.6

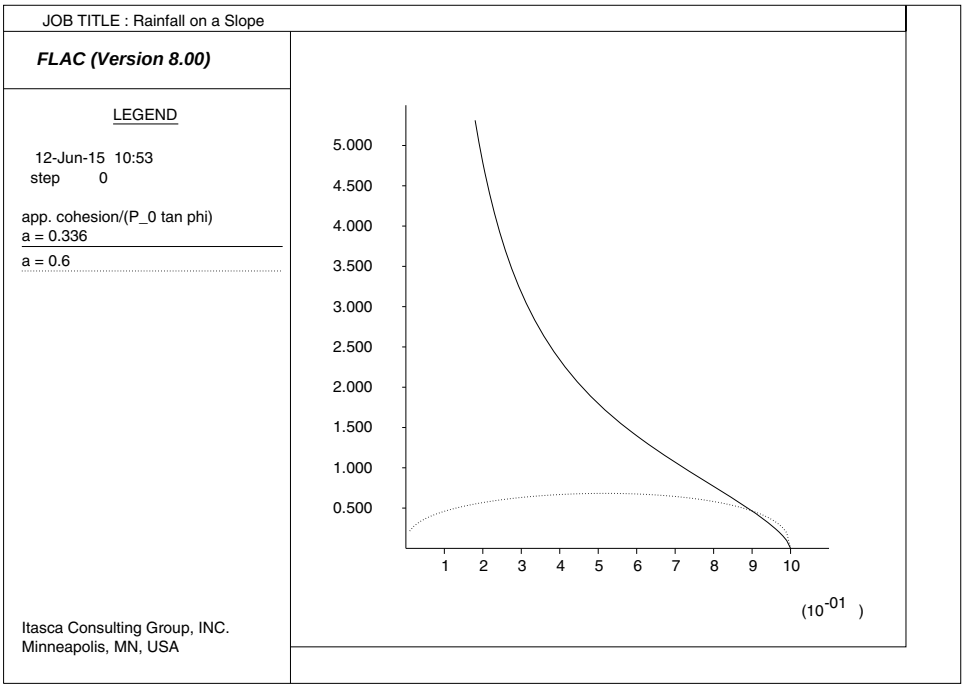

Figure 16.3 Cohesion curves, $C_c/(P_0 \tan\phi)$ versus effective saturation, S_e, for a = 0.336 and a = 0.6

16.2.2 Steady-State Saturation and Pore Pressure

For this example, we will initially consider the state of a slope under a constant, long-term background infiltration from precipitation. Saturation and pore pressure estimates used for model initialization are calculated as follows.

The steady-state saturation for a given level of precipitation, q, may be estimated by considering a medium of large vertical extent (compared to the square root of intrinsic permeability $\sqrt{k\mu}$, where μ is dynamic viscosity of water). The gradient of pore pressure in the direction of gravity is negligible in that case, and the transport law simplifies to

$$q = k\kappa^{w}(S_w)\rho_w g \tag{16.6}$$

where k is the isotropic mobility coefficient, and for the case of zero residual saturation, the relative permeability, κ^{w}, is given by (see Section 2.2.1 in **Fluid-Mechanical Interaction**)

$$\kappa^{w} = S_w^b\left[1-(1-S_w^{1/a})^a\right]^2 \tag{16.7}$$

The parameters a and b in the law are determined experimentally. After substitution of Eq. (16.7) into Eq. (16.6), we obtain the equation

$$S_w^b\left[1-(1-S_w^{1/a})^a\right]^2 = \frac{q_1}{\rho_w g k} \tag{16.8}$$

This equation can be solved for S_w to provide the estimate of initial (steady-state) saturation.

Also, the water pressure in the unsaturated zone (referred to as soil suction in the literature) is given in terms of saturation by the capillary law. For zero residual saturation (and atmospheric air pressure), the van Genuchten form of the law is (see Eq. (16.5))

$$-P_w = P_0\left[S_e^{-1/a}-1\right]^{1-a} \tag{16.9}$$

This formula can be used to calculate (negative) initial pore pressure from known initial saturation and reference capillary pressure, P_0.

16.3 Modeling Procedure

The *FLAC* analysis for this example is performed using the two-phase flow configuration (**CONFIG tpflow**) in order to evaluate the effect of capillary pressures. (The project file for this model is "rainfall.prj".) The slope geometry and *FLAC* grid for the simulations are represented in Figure 16.4. The model is 60 m wide, the highest elevation from the base is 30 m (left side of model), and the shortest is 10 m (right side of model). The flat part of the valley, included in the model, is 20 m wide.

The slope is composed of silty soil, which is modeled as a Mohr-Coulomb material with zero cohesion and a 30° friction angle. The material and fluid properties assumed for this problem are listed in Table 16.1. The wetting fluid is water, and the non-wetting fluid is air.

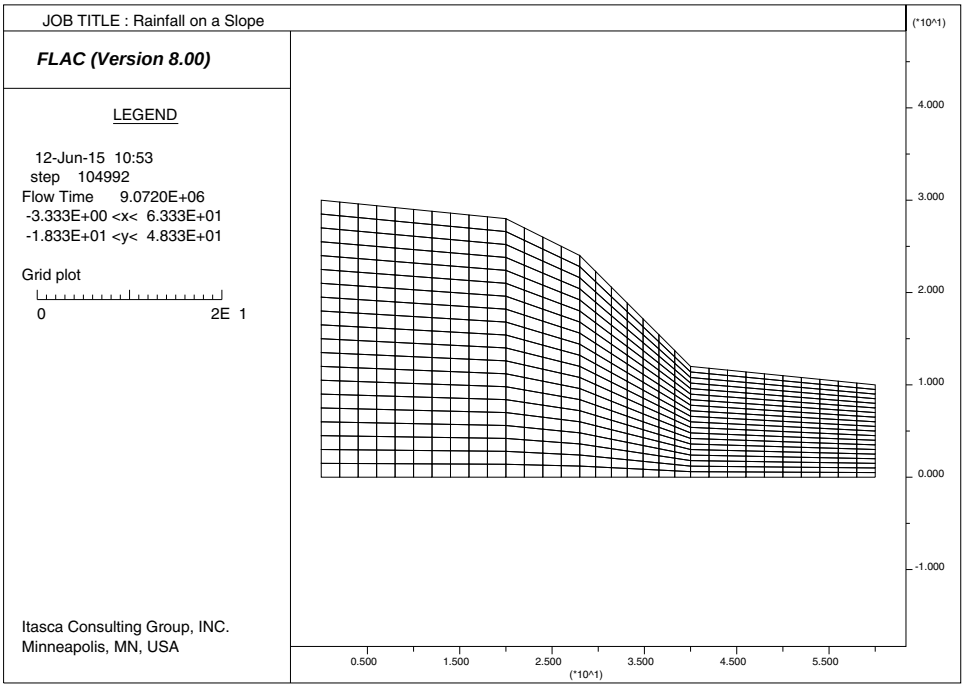

Figure 16.4 FLAC grid

The capillary and cohesion curves for the parameters assumed in the model are represented by the top curves in Figures 16.2 and 16.3. The slope is lying at an angle (45°) higher than the angle of repose (30°). If the material were completely dry, the slope would fail. However, for our analysis, we assume that the material was partially saturated at the time of formation of the slope (see note about silty material saturation behavior in Section 16.2). Also, partial saturation is maintained by a steady background precipitation at a rate, q_1, of 3.3 inches/month (84 mm/month).

Table 16.1 Soil and fluid properties for slope

Soil	
Dry density (kg/m^3)	2000
Drained bulk modulus (MPa)	200.0
Shear modulus (MPa)	100.0
Drained cohesion (Pa)	0
Drained friction angle (degrees)	30
Dilation angle (degrees)	0
Mobility coefficient (m^2/(Pa-sec))	10^{-9}
Porosity	0.1
Fluid	
Wetting fluid density (kg/m^3)	1000
Non-wetting fluid density (kg/m^3)	0.0
van Genuchten parameter, a	0.336
van Genuchten parameter, b	0.0
van Genuchten parameter, P_0 (MPa)	0.015
Wetting fluid modulus (MPa)	1.0
Non-wetting fluid modulus (Pa)	1.0
Undrained coefficient	0.0
Residual saturation	0.0
Viscosity ratio	1.0

For an infiltration rate of 84 mm/month (3.220×10^{-8} m/sec), and the property values listed in Table 16.1, the steady-state saturation is evaluated from Eq. (16.8) to be approximately 0.54. Because the relative permeability for water is an increasing function of water saturation, the steady-state saturation will be larger for larger infiltration rate, as expected. For an infiltration rate of 228 mm over four days (6.615×10^{-7} m/sec), the steady-state saturation is evaluated from Eq. (16.8) to be approximately 0.836.

In Section 16.2 it was shown how, in the framework of our analysis, a change in saturation (e.g., between two consecutive rainfall events) directly affects the value of apparent soil cohesion, C_c. This observation can be used to evaluate the potential impact of a change in saturation on stability of the slope.

This simulation is run in three stages. First, the initial steady-state flow condition is calculated for a constant infiltration rate of intensity of 84 mm/month. Then, the first rainfall event is modeled to simulate a rainfall accumulation of 584 mm (23 inches) over seven months. Finally, a second rainfall event of 228 mm (nine inches) over four days is simulated. An uncoupled analysis is performed for the first two stages, in which the wetting fluid modulus is reduced to 0.1 MPa in order to speed the calculation. A coupled analysis is performed for the third stage, with the fluid modulus set to the actual value of 1 MPa.

16.4 Results and Discussion

16.4.1 Initial Conditions

The initial conditions for the *FLAC* simulations correspond to steady-state flow with a constant infiltration rate of intensity q_1 (84 mm/month). Also, initially, the base of the model includes a saturated region with thickness of approximately 1 meter (below the so-called water table). To speed the calculation process, the initial (steady-state) saturation for the rate q_1 is estimated from Eq. (16.8), and the value (0.54) is assigned to the model. Also, a corresponding water pressure is derived from the capillary pressure law Eq. (16.9), and assigned as an initial value in the model (the value is -45.2 kPa).

To account for the presence of the initial phreatic surface in the model, we use an artificial calculation scenario, at the end of which the saturated aquifer thickness is roughly 1 meter. In this scenario, the bottom and lateral sides of the model are kept impermeable, and a constant infiltration rate of intensity q_1 is applied for an appropriate time period. The constant infiltration, q_1, is applied along the slope face using **APPLY discharge** commands with adjustments to account for the slope angle. (See "ADJUST_DISCHARGE.FIS".)

During the calculation, saturation and water pressure remain equal to their initialized value in most of the unsaturated region, except for a transition zone above the phreatic surface. The resulting (consistent) pore-pressure distribution is plotted in Figure 16.5.

The model is then run to mechanical equilibrium under gravity. Roller boundary conditions are used on the lateral sides of the model, and fixed (x and y) displacements at the base. Contours of vertical stresses at the initial stage are plotted in Figure 16.6.

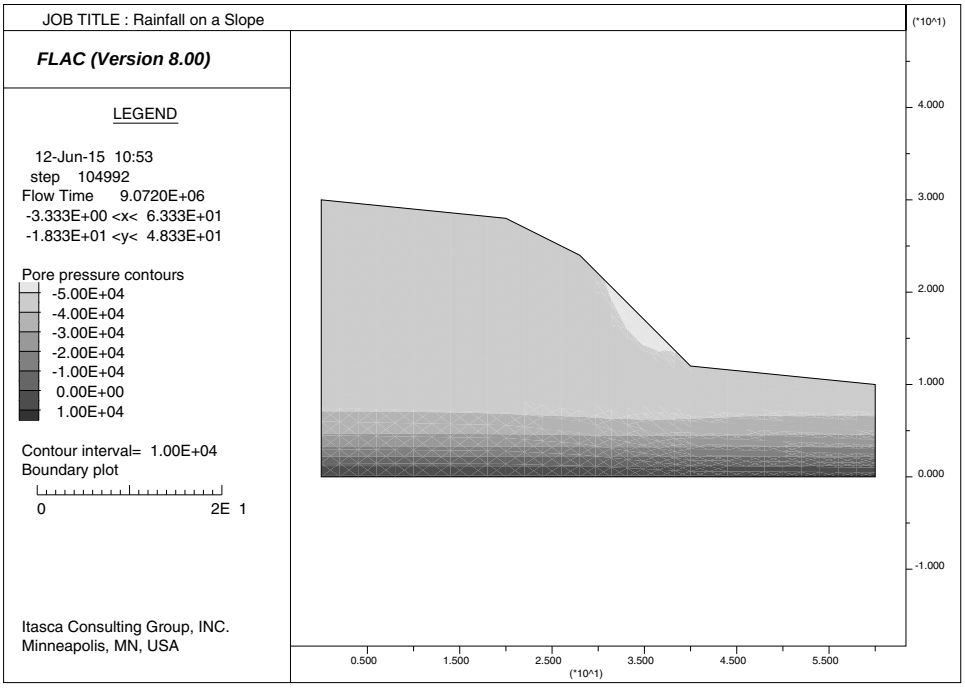

Figure 16.5 Initial pore pressure distribution at steady state

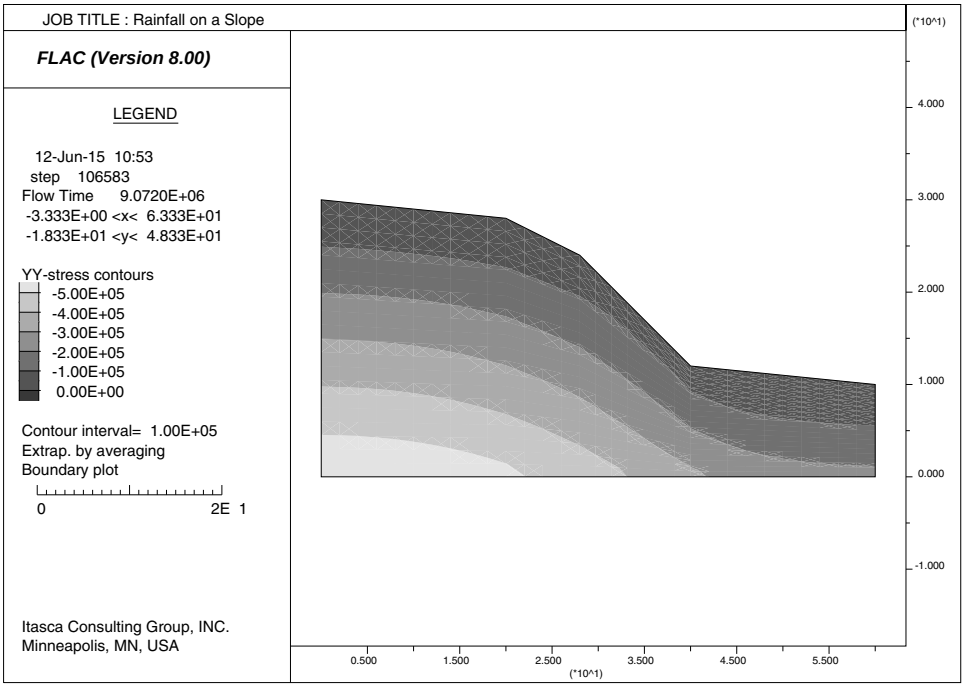

Figure 16.6 Initial vertical stress state

16.4.2 First Rainfall Event: Low Intensity, Long Duration

Starting with the initial conditions (established above), the pore pressure is fixed over the saturated part of the aquifer on the right side of the model (height of 1 meter), while the left side of the model is kept impermeable. The discharge of intensity q_1 (84 mm/month) is applied on the top surface of the model for 7 months, to reach a cumulative precipitation of 0.588 m (23 inches) over that period. The pore pressure distribution at the end of the 7 consecutive months of rainfall is shown in Figure 16.7. Contours of saturation at the end of the first rainfall event are plotted in Figure 16.8 (saturation = 1 is fully saturated).

The saturation remains fairly uniform and equal to the steady state value over the major part of the slope. This is because the saturated height of the aquifer towards the left side of the model has increased by less than 3 m over the last 7 months duration of the rainfall event. Also, the problem response is dominated by gravity, and the thickness of the transition zone (where saturation evolves between the steady state value to one) is relatively small. The capillary parameter, $\eta = P_0/(\rho_w g)$ = 1.5 meter, is a small value compared to the maximum model height of 30 meters.

The model is then run to mechanical equilibrium. Displacement vectors are shown in Figure 16.9. The slope is still stable at the end of the first rainfall event.

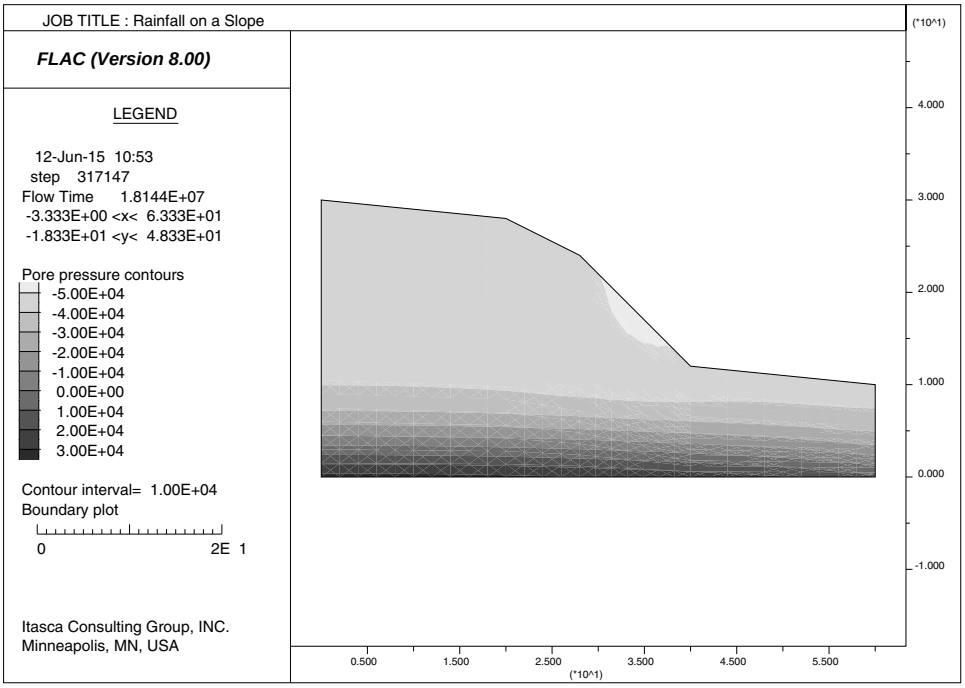

Figure 16.7 Pore pressure distribution after first rainfall event

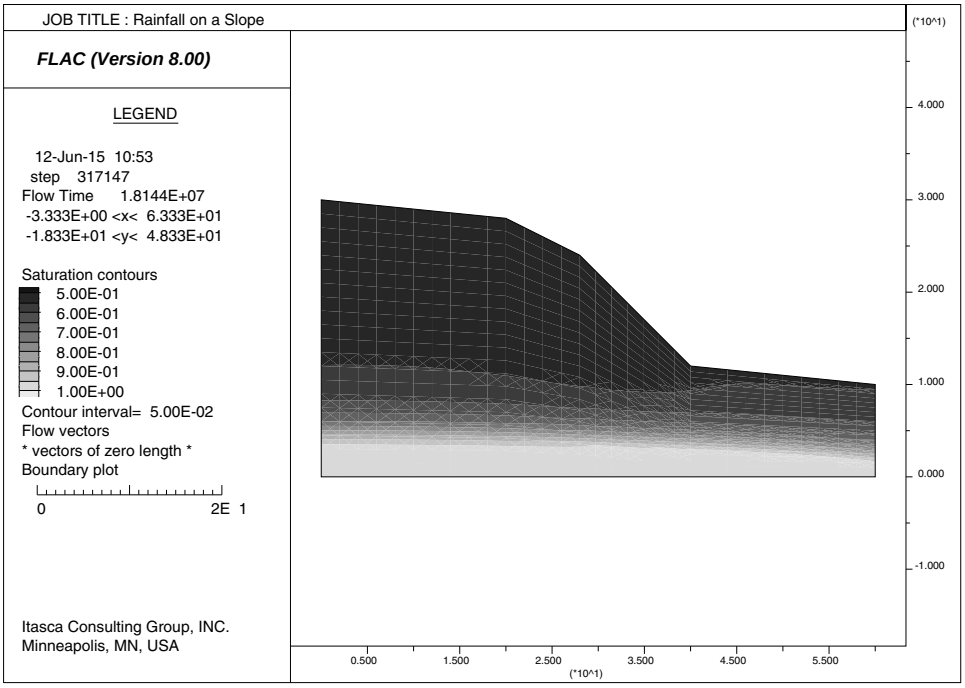

Figure 16.8 Saturation contours after first rainfall event

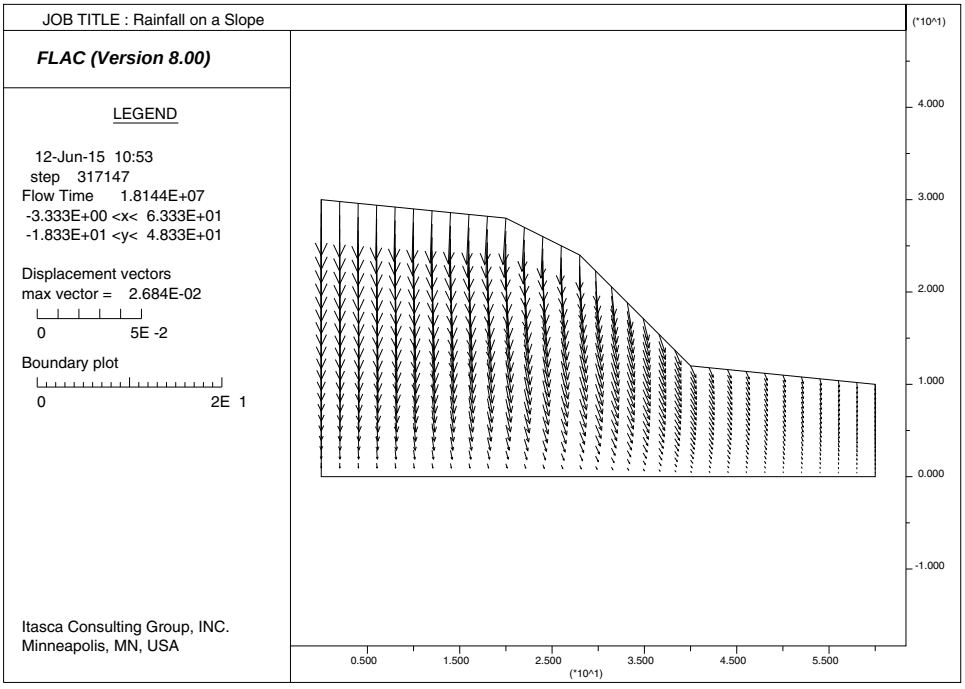

Figure 16.9 Displacement vectors after the low-intensity, long-duration rainfall event

16.4.3 Second Rainfall Event: High Intensity, Short Duration

The second rainfall event corresponds to an additional 228 mm (nine inches) of rainfall over a period of four days. A coupled numerical simulation is conducted to cover the time scale of this event. The slope is failing in this case. The velocity vectors at the end of the simulation are shown in Figure 16.10. Contours of saturation and flow vectors are shown in Figure 16.11.

Saturation at the ground surface is seen to increase toward a new steady state value (0.836), consistent with the higher magnitude of the current rainfall event. The increase of saturation is responsible for the subsequent reduction in apparent soil cohesion, and ultimate failure of the slope.

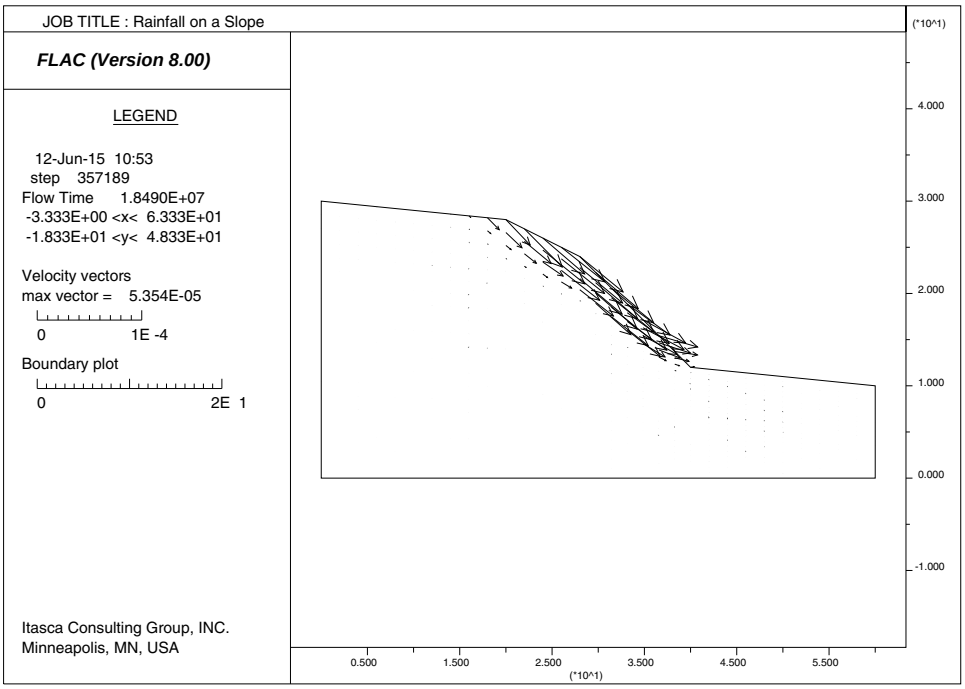

Figure 16.10 Velocity vectors after the high-intensity, short-duration rainfall event

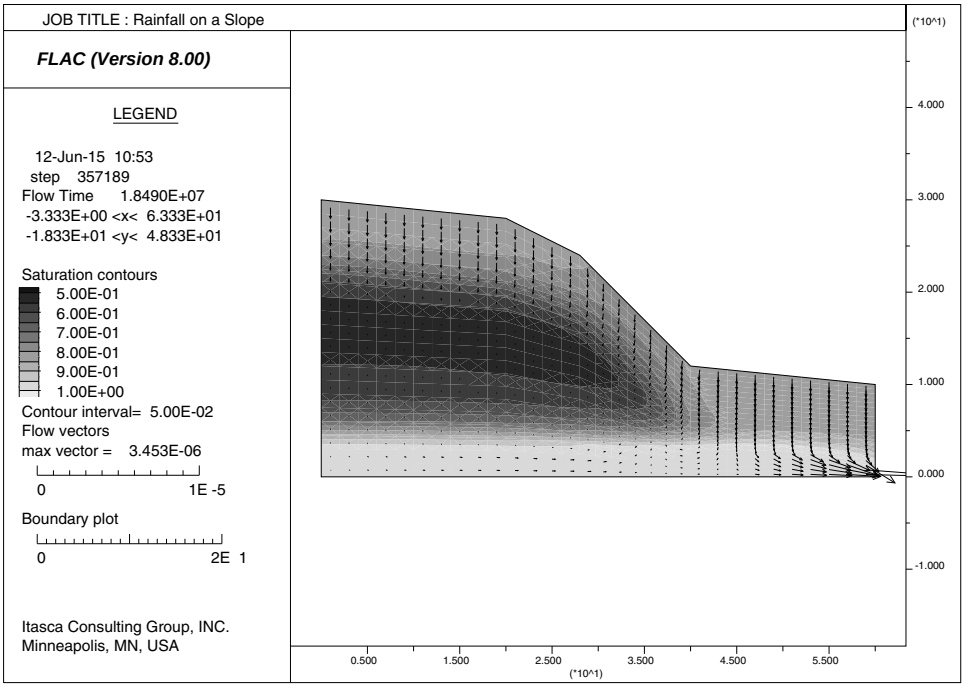

Figure 16.11 Saturation contours and flow vectors after the second rainfall event

16.4.4 Discussion

Coupled numerical simulations of unsaturated seepage flow were performed to show the impact of intensity and duration of a rainfall event on the stability of a slope. Generic geometry and material properties were used for the slope. It was shown that a rainfall event of low intensity and long duration was not detrimental to slope stability, provided the additional cohesion provided to the soil by the capillary forces was sufficient. On the other hand, a rainfall event of high intensity and short duration was responsible for slope failure. In this case, the behavior was explained by an increase in soil saturation, accompanied by a decrease in the capillary forces intensity, causing an apparent decrease in soil cohesion.

16.5 Reference

Bear, J. ***Hydraulics of Groundwater***. New York: McGraw-Hill (1979).